Continuous detection of extracellular ATP on living cells by using atomic force microscopy

Stefan W. Schneider*†‡, Marie E. Egan§, Bhanu P. Jena*, William B. Guggino¶, H. Oberleithner‡, and John P. Geibel*†‖

Departments of *Surgery, †Cellular and Molecular Physiology, and §Pediatrics, Yale University School of Medicine, New Haven, CT 06520; ¶Departments of Physiology and Pediatrics, John Hopkins University School of Medicine, Baltimore, MD 21205; and ‡Department of Physiology, University of Muenster, D-48149 Muenster, Germany

Communicated by Robert W. Berliner, Yale University School of Medicine, New Haven, CT, August 2, 1999 (received for review November 5, 1998)

Atomic force microscopy is a powerful technique used to investigate the surface of living cells under physiological conditions. The resolution of the instrument is mainly limited by the softness of living cells and the interactions with the scanning tip (cantilever). Atomic force microscopy, in combination with myosin-functionalized cantilevers, was used in the detection of ATP concentrations in solution and on living cells. Functionally active tips were used to scan the surface of cells in culture and to show that the CFTR+ cell line (S9) had a basal surface ATP concentration that could be detected with atomic force microscopy ($n = 10$). ATP-dependent signals were not detectable in cells scanned with noncoated or heat-inactivated enzyme-coated tips ($n = 9$). Enzymatically active tips may serve as a model for future development of atomic force microscopy biosensors that can simultaneously detect topographical and biologically important compounds at the surface microenvironment of living cells.

CFTR cell line | atomic force microscopy

The role of intracellular ATP as an energy source and its complex biochemical interactions with living cells have been the focus of extensive research (1, 2). A natural progression of this research has lead investigators to speculate on the function of extracellular ATP in biological processes. The potential regulatory effects of extracellular ATP on platelet aggregation (3), vascular tone (4), muscle contraction (5), the generation of pain signals (6), and the ion channel (7–11) have been the foci of numerous in-depth studies. One of the most difficult problems associated with this research is the ability to detect and localize extracellular ATP on living cells accurately. Atomic force microscopy (AFM; ref. 12) can be used to measure topological changes on the surfaces of living cells at ultrahigh resolution (nanometer scale; ref. 13–17). This technique has been used to assay the morphology of living cells and the dynamic changes that occur after manipulations in the physiological environment surrounding the cell (18, 19). Recent studies have shown that AFM can be used as a viable tool to measure elasticity, enzyme activity, or chemically distinct functional groups after chemical treatment of AFM tips (20–24). Moreover, AFM is used as a tool for measuring intermolecular forces between ligand and receptor or between antigen and antibody (25, 26).

Methods

Commercially available Si_3Ni_4 cantilever tips (Digital Instruments, Santa Barbara, CA) were initially coated with BSA (1 mg/ml) and then with the myosin subfragment S1 (Sigma) by incubation of the 0.06-N/m Si_3Ni_4 tip in a 1-μM S1 solution over 24 h. The cantilever assemblies were mounted on the BioScope (Digital Instruments) and washed for 5 min by immersion in a Hepes buffer solution (pH 7.4, room temperature).

Test of Tip Functionalization. An ATP solution (10 μl; 2–200 μM; Sigma) was added to the chamber (2,000-μl volume) and caused a reproducible detectable deflection of the tip ($n = 25$). The functionalized tips gave a dose-dependent response in a concentration range of 10–500 nM (see Figs. 2 and 3). Doses greater than 500 nM failed to effect any further significant tip deflection ($n = 10$). To confirm that the deflection signal is caused by ATP hydrolysis, a series of studies were conducted with ADP and ATPγS (Sigma). Neither ADP (10 nM to 1 mM; $n = 3$) nor ATPγS (10 nM to 1 mM; $n = 5$) could cause a cantilever deflection, confirming that the active hydrolysis of ATP was necessary to cause tip deflection. Addition of ATP to functionalized tips that had been exposed previously to ATPγS or ADP resulted in rapid tip deflections (see Fig. 3; $n = 8$). When functionalized tips were tested with a solution containing 10 nM caged ATP there was no apparent deflection of the tip ($n = 5$). Exposure to a 100-ms burst of light from a UV light source resulted in a rapid controlled rise in tip deflection, indicative of ATP release and subsequent hydrolysis ($n = 5$). Exposure to the UV light source in the absence of the caged compound had no effect on either functionalized or nonfunctionalized tips (see Fig. 3; $n = 7$).

ATP Hydrolysis at the Surface of a Functionalized Tip. To determine the fate of ATP in the presence of the S1 myosin-coated and uncoated cantilevers, the reaction was performed in the presence of [α-^{32}P]ATP. S1 myosin-coated and uncoated cantilevers were incubated in Hepes buffer (pH 7.4) containing 100 nM ATP. Incubation of the reaction mixture was performed at room temperature. After the experiment, 2 μl of the reaction mix was spotted on polyethyleneimine TLC plates, and nucleotides were resolved by performing TLC developed in 1 M LiCl (27). ATP, ADP, and AMP were run simultaneously as standards. Autoradiography was performed on the dried TLC plates (see Fig. 3). After autoradiography, the TLC plates were cut at the appropriate ATP and ADP positions. The 30-min control (uncoated tip) and experimental (S1-coated tip) lanes on the TLC plate were counted by liquid scintillation, and the percentage of total ATP hydrolyzed to ADP was estimated at approximately 20%. These experiments show a time-dependent hydrolysis of ATP in the presence of the S1 subfragment but little hydrolysis in its absence.

Model for ATP Hydrolysis and Detection in Solution. To characterize ATP hydrolysis by a functionalized tip, a local volume of solution must be defined. Because the myosin subfragment is bound to the tip, a reasonable solution volume would be the microenvironment of the AFM tip. The shape of our tip is pyramidal with a 4-μm face in all directions. The local volume is then modeled as a sphere with a diameter of 4 μm, which would yield a volume of 2.4×10^{-14} liters (see schematic model in Fig. 1). The AFM tip, packed with the ATPase S1, moves into this area of high concentration and will contact the locally accumulated ATP

Abbreviation: AFM, atomic force microscopy.

‖To whom reprint requests should be addressed. E-mail: john.geibel@yale.edu.

The publication costs of this article were defrayed in part by page charge payment. This article must therefore be hereby marked "*advertisement*" in accordance with 18 U.S.C. §1734 solely to indicate this fact.

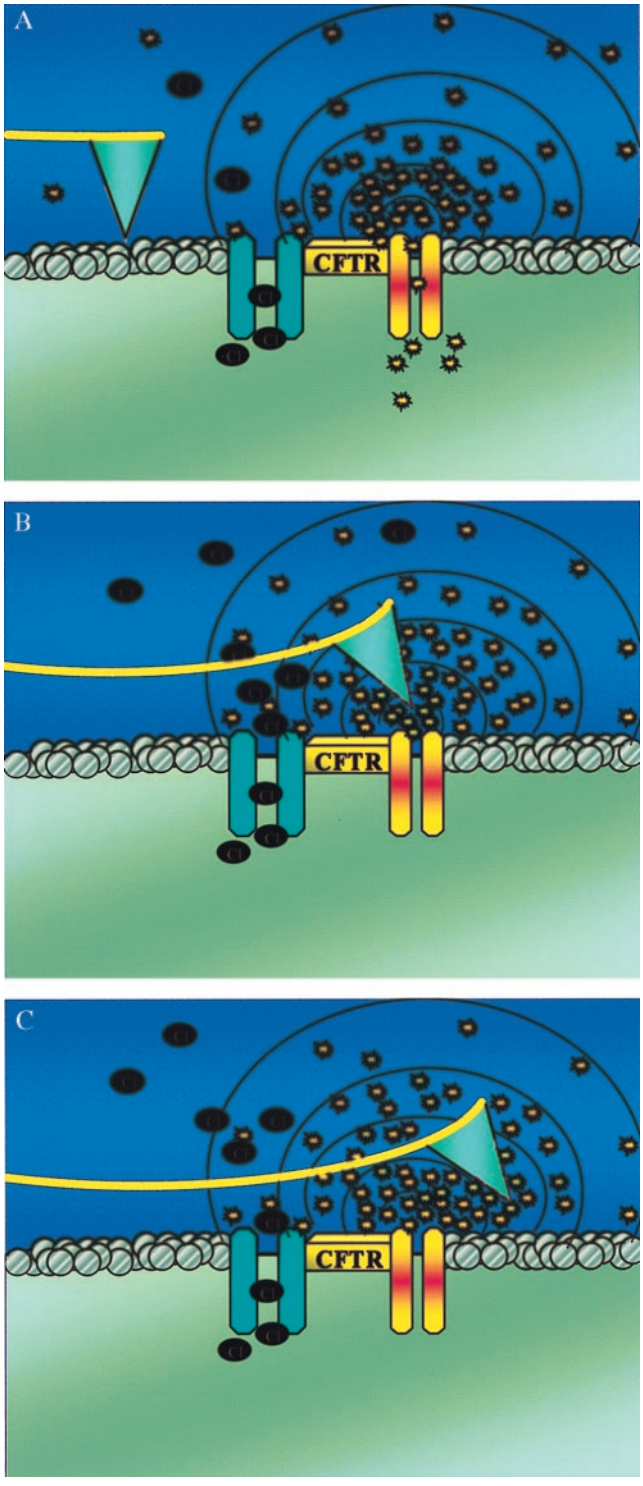

Fig. 1. (*A*) Schematic drawing of a functionalized S1 AFM tip imaging the extracellular surface of a CFTR expressing cell. Cl^- and ATP are released in the area adjacent to the CFTR protein. The black dots represent the chloride ions, and the yellow bursts are the ATP molecules. (*B*) ATP molecules bind to the tip. As the enzyme hydrolyzes ATP to ADP, there is a positive deflection of the tip. The tip remains deflected as long as ATP hydrolysis continues at the tip interface. (*C*) After passing the point source of ATP release, the tip remains in a deflected mode because of the short contact time (20 ms) compared with the ATPase activity time (≈300 ms).

molecules for about 20 ms. Calculating the local concentration for this very small volume, we can determine that 24 ATP molecules would yield a final concentration of 10 nmol/liter. This concentration is sufficient to get a significant ATP signal (see Fig. 3; $n = 8$). Of course, this calculation is true only as long as there is no change in ATP concentration because of local ATP hydrolysis. We have shown that, in our control experiments, we have a 10 nmol/liter concentration in 2 ml of control solution (i.e., an ATP pool of 2×10^{12} ATP molecules). However, the AFM tip is in contact with this local ATP pool for only 20 ms, which means that ATP hydrolysis will occur only one or two times while in this area of concentrated ATP. As mentioned above, as soon as our AFM tip comes into an area of high ATP, it will bind some ATP molecules and hydrolyze them by the ATPase S1. By coating the AFM tip with the S1 enzyme, we bring the enzyme into close proximity to the plasma membrane and the locally high ATP concentration. The direct contact area between cell surface and AFM tip has a diameter of about 400 nm; therefore, many individual enzymes (up to ≈600 individual enzymes) will be in close proximity to the local source of ATP release. After ATP binding to the S1 enzyme located at the AFM tip, ATP hydrolysis occurs. During hydrolysis, a conformational change of the enzyme occurs, which is in the range of 10 nm (28). Such conformational changes apparently disturb the interaction between the tip and the cell surface. This disturbance causes a measurable deflection that was detected as a bright line, indicative of a height change in our experiments (Fig. 2; see also Fig. 4). Recently, it was shown that a conformational change (in the range of <1 nm) of single molecules attached to the AFM tip could result in a measurable signal (14).

Quantification of the ATP Concentration on the Cell Surface. A volume adjacent to the plasma-membrane surface defined by the shape of a half sphere with a diameter of 200 nm requires only one ATP molecule to yield a final concentration of 1 μmol/liter. We need five ATP molecules in a half sphere with a diameter of 2 μm to get a concentration of 10 nmol/liter. A half sphere with a diameter of 4 μm requires 25 ATP molecules to yield a final concentration of 10 nmol/liter. A half sphere with a diameter of 20 μm requires 4,000 ATP molecules to get a concentration of 10 nmol/liter. Finally, in a medium with a volume of 2 ml, we need about 10^{13} ATP molecules to arrive at a concentration of 10 nmol/liter. From this model, it is apparent that leaving the local point source of ATP will have an immediate loss of a significant (measurable) ATP concentration within the volume surrounding the tip (Fig. 1).

Cell Culture. The S9 cell line is an airway epithelial cell line that stably expresses wild-type CFTR. The S9 cell line is derived from the IB3-1 cell line. The IB3-1 cell line is an immortalized, well characterized human bronchial epithelial cell line derived from a cystic fibrosis patient (29). Genotypically, the cell line is a compound heterozygote containing the ΔF508 mutation and a nonsense mutation, W1282X, with a premature termination signal. IB3-1 cells were transfected with adeno-associated virus wild-type CFTR containing vectors. These stably transfected IB3-1 cells, S9 cells, have a "corrected" Cl^- channel profile, in that they have a small linear CFTR Cl^- conductance and normal regulation of outwardly rectifying Cl^- channels as described (30, 31).

Cells were cultured as described in detail (10, 30, 31). Briefly, S9 cells were grown at 37°C in 5% CO_2 in LHC-8 medium (Biofluids, Rockville, MD) supplemented with 5% (vol/vol) FCS, 20 μg/ml gentamicin, 100 units/ml penicillin, and 100 μg/ml streptomycin. Cells were grown in culture flasks or glass chips coated with 150 μg/ml collagen, 10 μg/ml fibronectin, and 10 μg/ml BSA. Cells are passaged every 5–7 days.

In all studies presented, n is equal to the total number of dishes of cells scanned for each protocol, a minimum of two cells per dish were scanned.

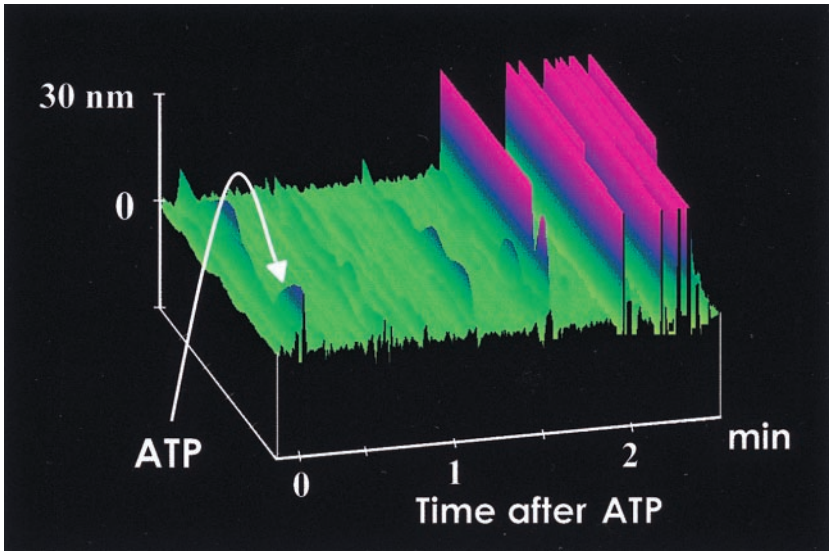

Fig. 2. Functionalized S1 tip scanning the surface of mica in fluid. After the addition of ATP (10 nM) indicated by the arrow, the tip starts to deflect after a time lag of 1–2 min because of diffusion of ATP toward the AFM tip. Tip deflections are shown in pink, whereas the mica surface is shown in green.

Results

In these studies, we have been able to use of the AFM as both a morphological instrument and a biosensor to detect extracellular ATP in the microenvironment of living cells directly (n = 13). The myosin (520 kDa) subfragment S1 (105 kDa), which contains the reactive ATPase portion of myosin, was chosen as our detection molecule because of its high affinity for ATP. We chose commercially available AFM tips, which were functionalized with the myosin subfragment S1 before use.

To test for functionalization at the tip for use in both surface topography measurements and ATP detection, tips were mounted in the BioScope holder (Digital Instruments) and positioned over the cell preparations by using an inverted microscope.

Tips were assayed for activity before cell scanning by exposure to a solution that contained 10^{-8} M caged-ATP or 10^{-8} M ATP. The deflection of the cantilever after hydrolysis of the ATP confirmed a functionalized tip, which was then used for the cell studies. Each functionalized tip was tested before use with cells and then after scanning the cells to confirm that the tip was still capable of detecting ATP at the same magnitude achieved before cell scanning. Fig. 1 *A–C* shows a schematic representation of a functionalized tip during cell-surface imaging and ATP hydrolysis. It is likely that the conformational change of the myosin ATPase induces a disturbance of the interaction between the AFM tip and the surface. The AFM feedback loop tries to compensate for this disturbance, which takes time. A typical image taken with a myosin-S1-functionalized tip is shown in Fig. 2 in the presence of ATP in the bath solution (n = 8). The hydrolysis of ATP by the S1 fragment results in increased deflections of the tip. The duration of the myosin displacements depends on the ATP concentration; the average time of the displacements increased as the ATP concentration decreased (31). Therefore, an ATP concentration of 1 μmol/liter or 10 μmol/liter induced displacement durations of around 260 ms and 72 ms, respectively. After 260 ms, the tip had moved around 10 μm (scan size of 40 μm; scan rate of 1 line per s). Thus, as the tip is finishing a deflection cycle, because of activation and deactivation, the tip has moved beyond the actual point source for ATP release and has continued to travel along the same line. The tracing then shows a "streak" as we come into this area of increased concentration and then continues to give a reaction reading after leaving the source for ATP because of the transient time for deactivation, which depends on the initial concentration. In the present study, we determined that our functionalized tips could detect concentrations of ≥10 nM ATP (n = 8). Confirmation of ATP consumption by the tip was established by radioactively labeled ATP hydrolysis measurements with myosin subfragment S1-functionalized tips (Fig. 3*D*; n = 3).

Detection of ATP on the Cell Surface. A cystic-fibrosis-affected airway epithelial cell line (30) that has been transfected with wild-type CFTR (S9) was used for this study. The S9 transfection previously has been shown to possess a Cl^- channel with characteristics of a complemented cell line that actively expresses wild-type CFTR (10, 31). In addition, it has been shown that activation of CFTR in this airway epithelial cell line is associated with the release of ATP into the extracellular environment (10, 11). For studies involving the CFTR (S9) cell line, we attached functionalized tips to the BioScope holder and confirmed activity when they were exposed to ATP before cell scanning. A new thermostatically controlled chamber was used that allowed both rapid solution exchange and direct visualization of the cells on an inverted microscope. Functionalized tips were used in a bidirectional scan mode; on the initial pass, the cell surface was scanned in contact mode AFM, allowing a direct topographic display of the cell surface. The subsequent pass of the tip was performed over the same area in "lift mode" to allow detection of ATP in the extracellular microenvironment (n = 10). The lift mode disengages the tip from the surface and allows direct interactions with the microenvironment rather than with the attractive forces of the cell surface. Studies were conducted at a range of 100–300 nm above the surface in lift mode. Areas of ATP localization were detected as deflections in the scan profile (illustrated in Fig. 4 *A* and *B*). We observed that each cell contained distinct point sources or areas of high deflection that were dispersed across the cell surface in a random pattern (n = 10). These areas of deflection would correlate with a basal ATP release in the vicinity of the tip, which equates to a finite local ATP concentration. Local concentration is defined as detecting ATP in a very small area at the cell surface. The ATP that is released by the cell from a point source diffuses into the adjacent extracellular medium or is hydrolyzed by ecto-ATPases. There will be more ATP molecules in close proximity to this point

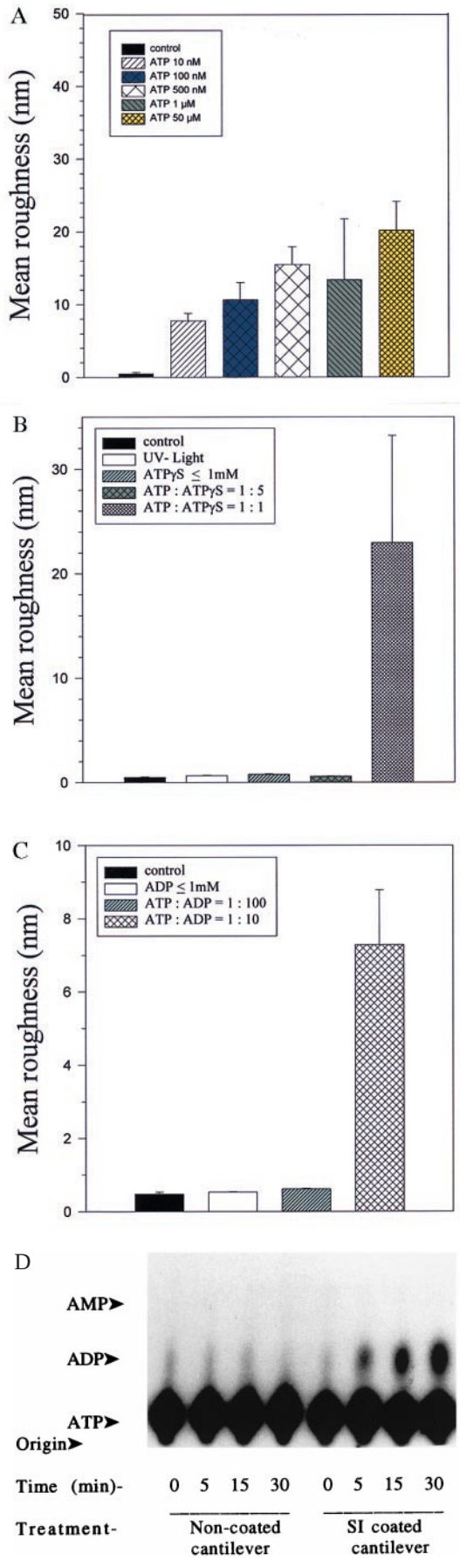

source compared with the number of molecules in a location away from the release point. The consequence is a concentration gradient related to the distance from the point source. The highest concentration will correlate to the source, where the ATP molecules are being extruded into the extracellular medium, with a rapid fall in concentration proportionate to the distance from the source because of the dilution into the larger volume (see Fig. 1). This calculated fall in concentration with distance explains the lack of activation of the tip in the medium, even during the sustained release of ATP in the immediate vicinity of the point source.

The activation of the tip therefore relies on reaching a sufficient concentration of ATP in a local volume in proximity to the tip (see *Methods* section). Applying this model of tip size and enzyme coating, it is possible to show that only a few ATP molecules (less than 100 ATP molecules) that are localized at the plasma membrane where the release occurs could be detected by a functionalized tip. In the entire bath chamber that has a volume of 2 ml, it would be necessary to have about 10^{13} ATP molecules to attain a concentration of 10 nmol/liter. These results again confirm why the functionalized tip does not activate in the dish with the cells; rather, activation (detectable tip deflection) occurs when the tip comes into proximity of the cell surface and the point source of ATP release.

This idea of small concentrated areas of extracellular ATP correlates with the proposed localization and frequency of the active CFTR complex in these cells (30, 32).

To demonstrate further that an active CFTR complex is necessary for the release of ATP into the extracellular environment, we attempted to block ATP secretion from the S9 cells. Glybenclamide, which has been shown to inhibit CFTR channel activity, was used in hopes of decreasing ATP concentration on the surface of the cells (10, 33–38). Monolayers of S9 cells were scanned initially with functionalized tips to identify areas of active ATP secretion (Fig. 4 *A* and *B*). After confirmation of hot spots along the cell surface, 10^{-4} M glybenclamide (10, 33–38) was added to the bathing medium ($n = 4$). As shown in Fig. 4 *A* and *B*, addition of 10^{-4} M glybenclamide reduced the ATP signal over time. This effect was not purely a time-associated event, because the addition of vehicle alone did not significantly reduce the deflectional activity of the tip and cell surface within the same time frame ($n = 6$). These data suggest that inhibition of CFTR is associated with a decrease in ATP release, which in turn decreased ATP at the extracellular surface of the cells. It should be noted that the areas of ATP on the surface did not appear as single spots but as a streaking pattern on the surface of the cells. Because of the nature of the scan pattern, the tip is not stationary but continuously moving across the surface of the cell in a linear scan pattern. As the tip encounters ATP, hydrolysis begins, and

Fig. 3. (*A*) Addition of different ATP concentrations to a functionalized AFM tip scanning mica in fluid is followed by dose-dependent deflection signals. The different concentrations are given in different colors and patterns. The corresponding deflection signals are given in the so-called mean roughness, a feature provided by the software package of the BioScope. The values expressed in nanometers represent the mean deviation of the data points in the plus and minus *z* direction in relation to a reference area set as zero (40). Mean roughness represents the mean value of the surface relative to the center plane (see also *B* and *C*). (*B* and *C*) After addition of the vehicle ATP-γS, which is unable to undergo hydrolysis, or ADP (*C*), we observe almost no change of the deflection signal illustrated by the lack of change in the mean roughness value. However, after addition of ATP (relative concentration to ATP-γS of 1:1 and to ADP of 1:10), an increase of the mean roughness can be detected. (*D*) Autoradiographs of a thin-layer chromatogram from a time course of [α-^{32}P]ATP hydrolysis in the presence of S1 myosin-coated and uncoated cantilevers. Note a time-dependent ATP hydrolysis in the presence of S1 myosin-coated cantilevers, which is not detected in the presence of uncoated cantilevers.

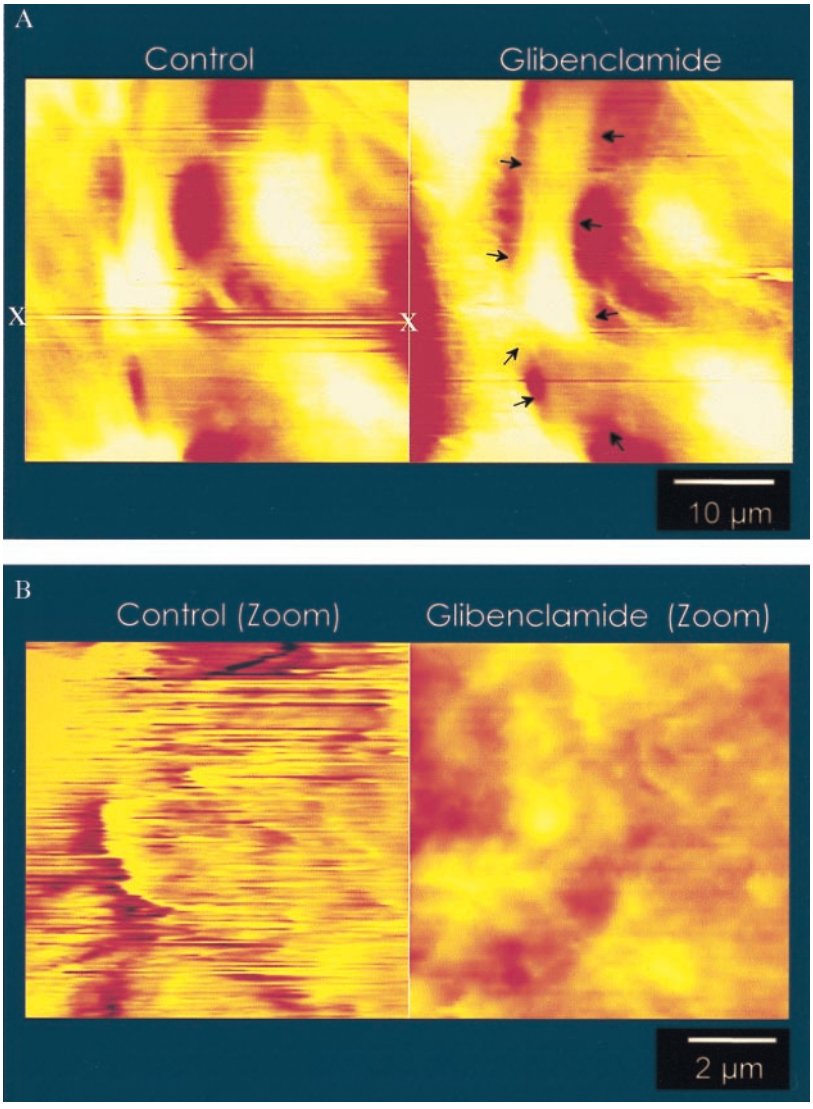

Fig. 4. Control scans of S9 cells with a functionalized AFM tip. (*A Left*) One ''hot spot'' of extracellular ATP (x) is clearly visible and reproducible over a time period of at least 30 min. These ATP pools are detectable as long streak lines (see x) at distinct locations along the surface of the cells in culture. The appearance of lines rather than points of deflections is caused by the rate of scanning (1–2 scan lines per s). The AFM tip first dips into a localized ATP pool and then moves away from this area as the scan progresses. As ATP hydrolysis occurs, a positive deflection of the tip is noted (illustrated in Fig. 1) causing a continuous line of activity. (*A Right*) The same cells after incubation with 10^{-4} M glybenclamide, a known inhibitor of CFTR. Note the reduction in hot spots (arrows), indicative of a reduction of extracellular ATP concentration. (*B Left*) High-resolution scan of a hot spot. Because of the localized ATP signal, the surface morphology of the cell is almost invisible. With increasing ATP levels at the cell surface, ATP hydrolysis by the S1 subfragment causes continuous deflections of the tip. The increased deflections caused by localized areas of high ATP activity reduce the ability to obtain the cell surface morphology. (*B Right*) For comparison, a cell after an incubation with 10^{-4} M glybenclamide.

the tip starts to deflect off the surface but continues to move, thus giving the impression of a streak. Typically, we found two to three areas of activity per cell scanned; all CFTR+ cells showed this activity pattern with a minimum of two to three areas per cell. Depending on its size, a scanned field could yield up to six areas of activation. If, however, the scan size is reduced, resulting in a concentrated repetitive scan over a small area, a profile pattern of ATP hydrolysis identical to that of the caged ATP controls occurs ($n = 5$).

In an additional series, S9 monolayers were exposed for 1 h to 10^{-4} M glybenclamide containing solution before scanning. After a 1-h exposure to glybenclamide, scan profiles of S9 cells lacked ''ATP-positive'' areas of activity and yielded scan profiles identical to non-CFTR expressing monolayers ($n = 3$). However, after removal of glybenclamide from the bath and exposure to 3-isobutyl-1-methylxanthine (100 μM) and forskolin (10 μM), stimulators of the CFTR protein and ATP release (10), the functionalized tips detected extracellular ATP along the surface of the previously nonresponsive cells (S.W.S., M.E.E., B.P.J., W.B.G., H.O., and J.P.G., unpublished observation). These studies provide additional evidence that the S9 cell line (CFTR expressing airway epithelial cell line) actively secretes ATP at its surface and that AFM functionalized tips can discern extracellular ATP in the microenvironment surrounding living cells under physiological conditions. As a positive control, we tested functionalized tips on the surface of nonexpressing CFTR cells and found that there was no activation of the tip when scanning the cell surface with the same parameters used with the CFTR expressing cells ($n = 3$). All tips had been tested for activity before scanning the cell surface. To confirm that the tips had maintained activity, the tips were again scanned after exposure

to the cell surface. All tips had maintained activity at similar levels before and after cell-surface scanning.

Discussion

These results represent an important innovation in the application of the AFM to biological preparations. The development of ATP-detecting tips is an example of modifying the scanning probe substrate to measure simultaneously high-resolution topography and a biologically important molecule in the surface microenvironment of living cells. This application is a further step in the development of a series of microbiosensors attached to the tip of the scanning stylus. This technique has been used successfully to detect ATP that has accumulated on the surface of a CFTR cell line. This result confirms the theory of active ATP secretion by these cells; furthermore, the ATP concentration along the surface can be influenced by either stimulation or inhibition of the CFTR regulatory protein on the apical membrane of the cell. Recently, Schwiebert and coworkers (39) were able to show, by using a bioluminescence method, a codetectable comparable concentration of ATP in the extracellular fluid. These studies predicted that there was a flux of ATP from the cell into the extracellular fluid; however, because of the technique used, they were unable to quantify the density of release sites or the area of release along the cell surface.

The successful implementation of the biosensor opens possibilities in the use of the AFM for a continuous live update of surface topography as well as a direct measurement of the microenvironment along the surface of the cell membrane in living cells under physiological conditions.

1. Gordon, J. L. (1986) *Biochem. J.* **233**, 309–319.
2. Dubyak, G. R. (1991) *Am. J. Respir. Cell Mol. Biol.* **4**, 295–300.
3. Macfarlane, D. E. & Mills, D. C. (1975) *Blood* **46**, 309–320.
4. Furchgott, R. F. & Zawadzki, J. V. (1980) *Nature (London)* **288**, 373–376.
5. Burnstock, G. (1972) *Pharmacol. Rev.* **24**, 509–581.
6. Chen, C. C., Akopian, A. N., Sivilotti, L., Colquhoun, D., Burnstock, G. & Wood, J. N. (1995) *Nature (London)* **377**, 428–431.
7. Stutts, M. J., Fitz, J. G., Paradiso, A. M. & Boucher, R. C. (1994) *Am. J. Physiol.* **267**, C1442–C1451.
8. Stutts, M. J., Chinet, T. C., Mason, S. J., Fullton, J. M., Clarke, L. L. & Boucher, R. C. (1992) *Proc. Natl. Acad. Sci. USA* **89**, 1621–1625.
9. Stutts, M. J., Lazarowski, E. R., Paradiso, A. M. & Boucher, R. C. (1995) *Am. J. Physiol.* **268**, C425–C433.
10. Schwiebert, E. M., Egan, M. E., Hwang, T. H., Fulmer, S. B., Allen, S. S., Cutting, G. R. & Guggino, W. B. (1995) *Cell* **81**, 1063–1073.
11. Al-Awqati, Q. (1995) *Science* **269**, 805–806.
12. Binnig, G., Quate, C. F. & Gerber, C. (1986) *Phys. Rev. Lett.* **56**, 930–934.
13. Henderson, E., Haydon, P. G. & Sakaguchi, D. S. (1992) *Science* **257**, 1944–1946.
14. Hoh, J. H. & Hansma, P. K. (1992) *Trends Cell Biol.* **2**, 208–213.
15. Schoenenberger, C.-A. & Hoh, J. H. (1994) *Biophys. J.* **67**, 929–936.
16. Parpura, V., Haydon, P. G. & Henderson, E. (1993) *J. Cell Sci.* **104**, 427–432.
17. Oberleithner, H., Giebisch, G. & Geibel, J. (1993) *Pflügers Arch.* **425**, 506–510.
18. Lal, R., Drake, B., Blumberg, D., Saner, D. R., Hansma, P. K. & Feinstein, S. C. (1995) *Am. J. Physiol.* **269**, C275–C285.
19. Barbee, K. A., Mundel, T., Lal, R. & Davies, P. F. (1995) *Am. J. Physiol.* **268**, H1765–H1772.
20. Radmacher, M., Cleveland, J. P., Fritz, M., Hansma, H. G. & Hansma, P. K. (1994) *Biophys. J.* **66**, 2159–2165.
21. Radmacher, M., Fritz, M., Hansma, H. G. & Hansma, P. K. (1994) *Science* **265**, 1577–1579.
22. Frisbie, C. D., Rozsnyai, L. F., Noy, A., Wrighton, M. S. & Lieber, C. M. (1994) *Science* **265**, 2071–2074.
23. Boland, T. & Ratner, B. D. (1995) *Proc. Natl. Acad. Sci. USA* **92**, 5297–5301.
24. Shroff, S. G., Saner, D. R. & Lal, R. (1995) *Am. J. Physiol.* **269**, C286–C292.
25. Florin, E.-L., Moy, V. T. & Gaub, H. E. (1994) *Science* **264**, 415–417.
26. Dammer, U., Hegner, M. & Anselmetti, D. (1996) *Biophys. J.* **70**, 2437–2441.
27. Jena, B. P., Brennwald, P., Garrett, M. D., Novick, P. & Jamieson, J. D. (1992) *FEBS Lett.* **309**, 5–9.
28. Finer, J., Simmons, R. M. & Spudnich, J. A. (1994) *Nature (London)* **368,** 113–118.
29. Zeitlin, P. L., Lu, L., Rhim, J., Cutting, G., Stetten, G., Kieffer, K. A., Craig, R. & Guggino, W. B. (1991) *Am. J. Respir. Cell Mol. Biol.* **4**, 313–319.
30. Flotte, T. R., Afione, S. A., Solow, R., Drumm, M. L., Markakis, D., Guggino, W. B., Zeitlin, P. L. & Carter, B. J. (1993) *J. Biol. Chem.* **268**, 3781–3790.
31. Egan, M. E., Flotte, T., Alfone, S., Solow, R., Zeitlin, P. L., Carter, B. J. & Guggino, W. B. (1992) *Nature (London)* **358**, 581–584.
32. Flotte, T. R., Afione, S. A. & Conrad, C. (1993) *Proc. Natl. Acad. Sci. USA* **90**, 10613–10617.
33. Sheppard, D. N. & Welsh, M. J. (1992) *J. Gen. Physiol.* **100**, 573–591.
34. Schultz, B. D., DeRoos, A. D. G., Venglarik, C. J., Singh, A. K., Frizzell, R. A. & Bridges, R. J. (1996) *Am. J. Physiol.* **271,** L192–L200.
35. Sheppard, D. N. & Robinson, K. A. (1997) *J. Physiol.* **503,** 333–346.
36. Sheppard, D. N. & Welsh, M. J. (1992) *J. Gen. Physiol*. **100,** 573–591.
37. McNicholas, C. M., Guggino, W. B., Schwiebert, E. M., Hebert, S. C., Giebisch, G. & Egan, M. E. (1996) *Proc. Natl. Acad. Sci. USA* **93,** 8083–8088.
38. Ruknudin, A., Schultze, D. H., Sullivan, S. K., Lederer, W. J. & Welling, P. A. (1998*) J. Biol. Chem.* **23,** 14165–14171.
39. Taylor, A., Kudlow, B. A., Marrs, K. L., Gruenert, D. C., Guggino, W. B. & Schwiebert, E. M. (1998) *Am. J. Physiol.* **274,** C1391–C1406.
40. Oberleithner, H., Schneider, S. W. & Henderson, R. M. (1997) *Proc. Natl. Acad. Sci. USA* **94**, 14144–14149.